

Soil moisture variations from boreal forests to the tundra

J. Kemppinen*¹, P. Niittynen*², T. Rissanen³, V. Tyystjärvi⁴, J. Aalto^{4,5} and M. Luoto⁵

* These authors contributed equally to this work.

¹ Geography Research Unit, P.O. BOX 8000, FI-90014 University of Oulu, Finland

² Department of Biological and Environmental Science, P.O. Box 35, FI-40014 University of Jyväskylä, Finland

³ Research Centre for Ecological Change, Organismal and Evolutionary Biology Research Programme, University of Helsinki

⁴ Weather and Climate Change Impact Research, Finnish Meteorological Institute, P.O Box 503, FI-00101 Helsinki, Finland

⁵ Department of Geosciences and Geography, P.O. Box 64, FI-00014 University of Helsinki, Finland

Corresponding author: Julia Kemppinen (julia.kemppinen@oulu.fi)

Key Points:

- Soil moisture was measured with 503 sensors in seven areas from April to September
- We found more spatial than temporal variation within the seven areas
- Soil moisture-topography relationships were time- and site-specific

18 **Abstract**

19 Soil moisture has a profound influence on life on Earth, and this vital water resource varies
20 across space and time. Here, we explored soil moisture variations in boreal forest and tundra
21 environments, where comprehensive soil moisture datasets are scarce. We installed soil moisture
22 sensors up to 14 cm depth at 503 measurement sites within seven study areas across northern
23 Europe. We recorded 6 138 528 measurements to capture soil moisture variations of the
24 snowless season from April to September 2020. We described the spatio-temporal patterns of
25 soil moisture, and test how these patterns are linked to topography and how these links vary in
26 space and time. We found large spatial variation and often less pronounced temporal variation in
27 soil moisture across the measurement sites within all study areas. We found that throughout the
28 measurement periods both univariate and multivariate models with topographic predictors
29 showed great temporal variation in their performance and in the relative influence of the
30 predictors within and across the areas. We found that the soil moisture-topography relationships
31 are site-specific, as the topography-based models often performed poorly when transferred from
32 one area to another. There was no general solution that would work well in all the study areas
33 when modelling soil moisture variation with topography. This should be carefully considered
34 before applying topographic proxies for soil moisture. Overall, these data and results highlight
35 the strong spatio-temporal heterogeneity of soil moisture conditions in boreal forest and tundra
36 environments.

37 **Plain language summary**

38 Water is fundamental for all life on Earth. Here, we investigated soil moisture of northern
39 environments, which is an important component in the global carbon cycle. We found large
40 spatial and temporal variations in soil moisture across the measurement sites within the seven

41 study areas. We found that the predictive power of the statistical soil moisture models varied
42 from site to site and week to week, which highlights the complexity of modelling soil moisture in
43 boreal forest and tundra environments.

44 **1 Introduction**

45 Soil moisture is a key component of the global water, energy, and biogeochemical cycles
46 (Koster et al., 2004; McColl et al., 2017; Oki et al., 2004; Seneviratne et al., 2010; Tuttle &
47 Salvucci, 2016). Across biomes, spatio-temporal soil moisture patterns are crucial for many
48 ecosystem functions and structures, such as primary production and decomposition (Green et al.,
49 2019; Hawkes et al., 2017; Hiltbrunner et al., 2012; Humphrey et al., 2021). In boreal forests,
50 soil moisture is strongly linked to photosynthesis, tree growth and survival, and forest fires
51 (Bartsch et al., 2009; D'Orangeville et al., 2016; Reich et al., 2018), and in the tundra, to
52 biodiversity, shrubification, and overall climate change impacts on ecosystem functions
53 (Ackerman et al., 2017; Bjorkman et al., 2018; le Roux et al., 2013). Overall, soil moisture is
54 crucial for plants and other soil dwelling organisms, as many species and their specific traits are
55 specialised for certain hydrological conditions (Lowry et al. 2011; Silvertown et al. 2015;
56 Kemppinen & Niittynen 2022). Pronounced spatial heterogeneity in soil moisture can thus be an
57 important agent in providing versatile habitats, and consequently, promoting biodiversity
58 (McLaughlin et al., 2017). Furthermore, temporal variation in soil moisture greatly affects
59 ecosystems, for instance, some species communities require more stable moisture levels than
60 others (Kemppinen et al. 2019). Therefore, data and analyses of soil moisture variations are
61 greatly needed to understand spatial and temporal variation in biological processes. Not least in
62 the context of climate change and biodiversity loss, this knowledge will help to identify efficient

63 strategies to adapt management and planning to reach important societal goals, such as
64 improving carbon sequestration, forestry practices, and biodiversity conservation and restoration.

65 The lack of soil moisture data poses a great uncertainty in estimating climate change
66 impacts on the global carbon cycle, to which boreal forest and tundra environments contribute
67 substantially (Chapin et al., 2000; Reich et al., 2018; Zona et al. 2022). Yet, field-quantified soil
68 moisture data from these environments are scarce (Dorigo et al. 2021). Anthropogenic climate
69 change shapes rapidly and drastically these northern environments (Post et al., 2019; Rantanen et
70 al. 2022). Along with the increasing air temperatures, precipitation variability and evaporation
71 are projected to increase, and the earlier onset of snowmelt can lead to summer and autumn time
72 drought (Bintanja et al., 2020; Rasmijn et al., 2018; Samaniego et al., 2018). Consequently, soil
73 moisture patterns are facing major changes across the northern hemisphere because water enters
74 the soil via precipitation (including snowfall), and is removed by runoff, infiltration, evaporation,
75 and transpiration (Western et al. 2002). These locally varying physical processes ultimately
76 shape the spatio-temporal variation of soil moisture, and are controlled by environmental factors,
77 such as topography, climate, soil, and vegetation (Albertson & Montaldo, 2003; Teuling, 2005;
78 Wilson et al., 2004). This means that the processes can increase and decrease soil moisture
79 variation from metre to metre and from day to day.

80 Topography is a static factor. Thus, relating it directly to such a dynamic phenomenon as
81 soil moisture can be problematic, and yet this is often done (Kopecký et al. 2021; Riihimäki et al.
82 2021), for instance, in ecological and biogeographical modelling (see e.g., Niittynen et al. 2018).
83 Topography-based variables, such as the Topographic wetness index (TWI), are commonly used
84 proxies for soil moisture (Western et al. 1999; Sorensen & Seibert 2007; Ågren et al. 2014;
85 Kopecký et al. 2021). Topography-based indices show temporal variation in their performance as

86 proxies for soil moisture; they perform better in wetter seasons (Western et al. 1999; Ali et al.
87 2013; Riihimäki et al. 2021). Topography is most strongly related to runoff (Beven & Kirkby,
88 1979), and to some extent, topography also influences the local spatial variation in infiltration
89 (via e.g., its effects on soil formation), evaporation (via microclimate), and transpiration (via
90 vegetation). All these processes vary greatly also in time. However, topography-based indices do
91 not contain any temporal information relevant for soil moisture, e.g., snow melt, precipitation,
92 evaporation, or transpiration (Crave & Gascuel-Oudoux 1997; Western et al. 1999; Wilson et al.
93 2004). Overall, it is insufficiently understood how the soil moisture-topography relationship
94 varies in different environmental contexts and points in time.

95 Here, we explore surface soil moisture across and within boreal forest and tundra
96 environments. We use temporally continuous soil moisture sensor data (up to 14 cm depth) from
97 503 measurement sites within seven study areas. The data range from April to September, which
98 is the snowless season in the study areas. The objectives of this work are to 1) describe the
99 spatio-temporal patterns of soil moisture across and within boreal forest and tundra
100 environments, and 2) test how these patterns are linked to topography and how these links vary
101 in space and time. Our aim is to describe the variability of soil moisture and its relationship with
102 topography across time and space.

103 **2 Materials and Methods**

104 **2.1 Study areas**

105 The seven study areas extended from southern Finland to northern Norway (Table 1,
106 Figure 1). The areas covered distinct Fennoscandian environments, that is, tundra, mires, and
107 forests, including hemi-, southern, middle, and northern boreal forests as well as sub-Arctic and

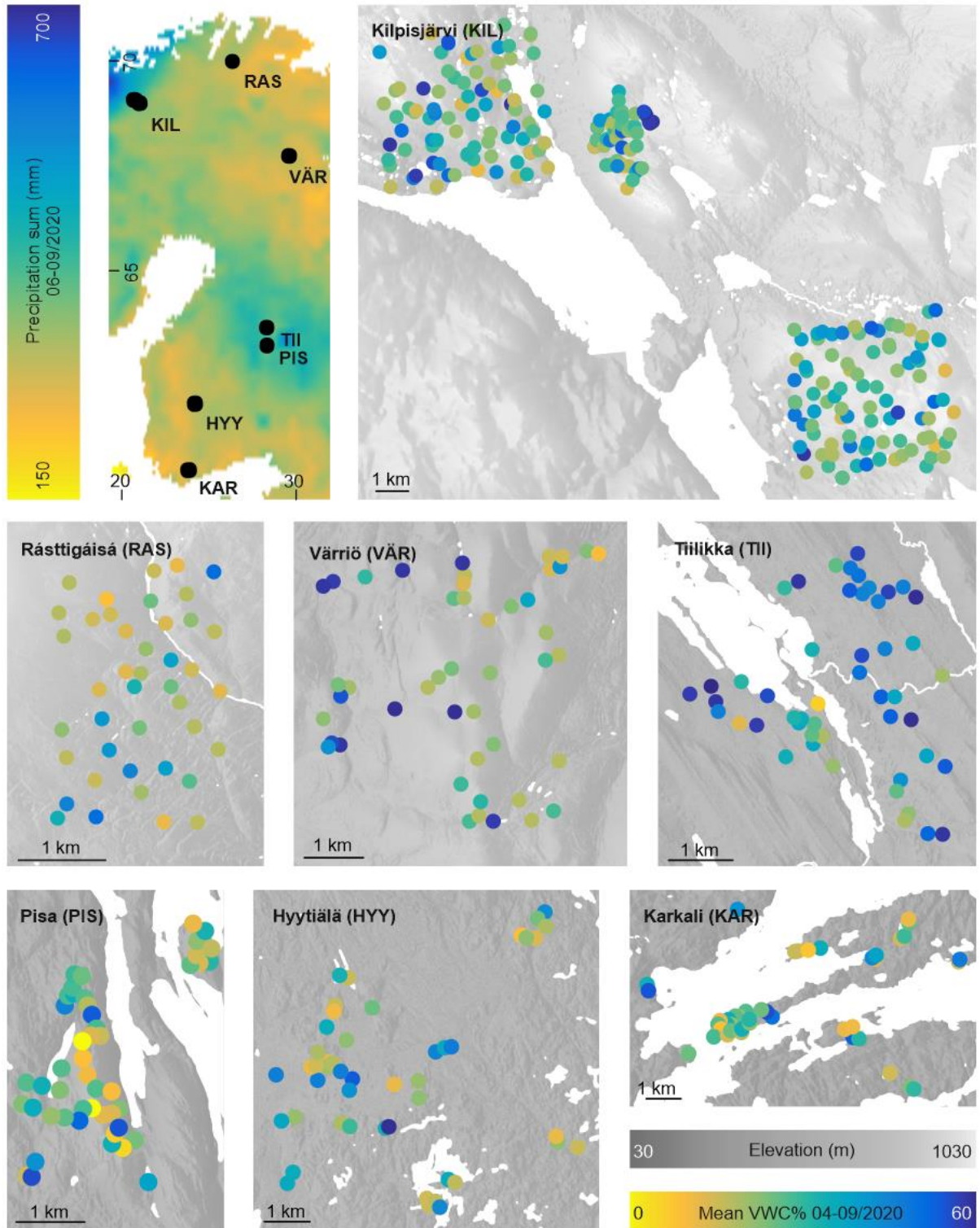
108 alpine tundra. The areas were located mainly in protected nature reserves with low anthropogenic
 109 influence (Table S1).

110 Table 1. Study area description. Each measurement site was equipped with a soil
 111 moisture sensor. Climate data was derived for years 1981-2010 from the nearest meteorological
 112 stations (Table S1).

Study area			Geography		Climate		Topography
Name	Size (km x km)	Sites (n)	Location (N, E)	Environment	Mean annual air temperature (°C)	Annual precipitation sum (mm)	Elevation (m)
Rásttigáisá	2x3	43	69.987, 26.345	Tundra	-1.3	433	400-763
Kilpisjärvi	15x15	227	69.062, 20.822	Tundra, northern boreal	-1.9	487	473-953
Värriö	5x5	46	67.736, 29.596	Tundra, northern boreal	-0.5	601	261-475
Tiilikka	4x5	49	63.646, 28.312	Middle boreal	2.3	591	169-231
Pisa	3x4	48	63.218, 28.328	Southern boreal	2.0	670	96-272
Hyytiälä	7x7	47	61.831, 24.196	Southern boreal	3.5	711	148-218
Karkali	9x6	43	60.248, 23.830	Hemiboreal	5.5	723	30-101

113 Rásttigáisá study area is entirely above the treeline and has a mountainous and
 114 heterogeneous relief. Kilpisjärvi is mainly heterogenous mountain tundra but the lowest valleys
 115 dip into the mountain birch forests. Värriö is mainly boreal forest with open wetlands along
 116 gently sloping landscapes but the highest peaks ascend above the treeline. Tiilikka is dominated
 117 by peat bogs and the relief is relatively flat. Pisa is remarkably hilly and dominated by Norway
 118 spruce forests at lower elevations and Scots pine forests at hill tops. Hyytiälä is a mix of boreal

119 forests and open wetlands and has relatively flat terrain. Karkali is a mix of broad-leaf forests
 120 (with temperate elements) and boreal needle-leaf forests in a relatively hilly terrain.



122 Figure 1. Spatial variation of soil moisture. Black points represent the seven study areas
123 across northern Europe. Coloured points represent the measurement sites and their mean soil
124 moisture values as volumetric water content (VWC%). The white polygons represent water
125 bodies. The precipitation data are based on the atmospheric reanalysis ERA5-Land by the
126 European Center for Medium-Range Weather Forecasts. Data sources for the terrain maps are
127 described in the Methods.

128 2.2 Measurement sites within the study areas

129 We conducted a random stratification to pre-select a suite of candidate measurement sites
130 to maximally cover the main environmental gradients within the seven study areas (Aalto et al.
131 2022). This was conducted separately for each study area, except for Rásttigáisá study area and
132 part of the Kilpisjärvi study area (see details below). The environmental variables that were used
133 to stratify the environmental space vary from study area to another based on the area-specific
134 characteristics but included variables such as total canopy cover, deciduous canopy cover,
135 distance to forest edge, altitude, potential incoming solar radiation, and a topographic wetness
136 index (SAGA wetness index) (Conrad et al., 2015).

137 In the random stratified site sampling methodology, first we masked the areas outside the
138 study areas and other unsuitable areas such as lakes and extracted the remaining pixel
139 information into a data frame. Next, we took a random subset of half of the remaining points
140 (i.e., pixels) and used this data to reduce the multidimensional environmental space into its first
141 three principal components with eSample function from iSDM R package (Hattab et al., 2017;
142 Hattab and Lenoir 2017). Then we took a sample of 100 points that maximally and
143 systematically covered the shrunk environmental space. Because these 100 points may be located
144 just next to each other, we repeated these procedures 100 times. Next, we pooled all the samples

145 and used the frequency of selection for each point as the weight in the final random selection of
146 points where we also kept a minimum distance of 100 m between the points. The final selection
147 of the points, that is the measurement sites, was visually inspected from the histograms of the
148 environmental variables. The final decision of each preselected measurement site was done in the
149 field, for instance, by skipping sites that were logistically challenging or were too similar with
150 other sites.

151 Selecting the measurement sites was carried out as described above, except for two study
152 areas; Rásttigáisá study area and part of the Kilpisjärvi study area. All measurement sites in
153 Rásttigáisá were based on a systematic study design (see additional material attached: manuscript
154 appendix from Rissanen et al. In preparation), in which the sites were chosen using a stratified
155 sampling based on elevation, potential incoming solar radiation, a topographic wetness index
156 (SAGA wetness index) (Conrad et al., 2015), snow cover duration, and soil quality to represent
157 main environmental gradients within the area. Some of the measurement sites (50/227 sites) in
158 Kilpisjärvi were based on a systematic study design (Kemppinen et al., 2018; Tyystjärvi et al.,
159 2021), which was complemented with sites in extreme soil moisture regimes (meltwater channels
160 and ridge tops), snow conditions (short and long snow cover duration), and elevations (near
161 mountain tops).

162 2.3 Soil moisture data

163 We measured soil moisture between 1.4.2020 and 30.9.2020 at all 503 measurement sites
164 located within the seven study areas (Figure 1). We used soil moisture sensors (TMS-4
165 dataloggers; TOMST Ltd., Prague, Czech Republic), which measure soil moisture to a depth of
166 c. 14 cm (Wild et al., 2019). We set the loggers to measure with a 15-minute interval. The time-
167 domain transmission method is used in the sensors to measure soil moisture (see Wild et al.,

168 2019 for a detailed description of the sensor and the measurement technique). In short, the
169 method is based on counting the number of electromagnetic pulses that travel within the counting
170 unit within a unit time, and this number informs about the moisture content of the soil (high soil
171 moisture decreases the number of pulses, low soil moisture increases them). The sensors produce
172 raw time-domain transmission data, which we converted into volumetric water content (VWC%)
173 using a conversion function adopted from Kopecký et al. (2021). We also tested conversion
174 functions presented in Wild et al. (2019), which are specific to different soil types. For this
175 purpose, we did a rough soil type classification in the field, where we assessed particle size of
176 the mineral soil and measured the depth of the organic soil layer. However, we noticed that these
177 soil type specific conversion functions resulted in highly unphysical VWC% values (e.g., $< 0\%$
178 and $> 100\%$), especially in peatlands. Thus, we concluded that the conversion functions in Wild
179 et al. (2019) are not applicable for the soil types present in our study areas, specifically, the
180 organic soils in boreal peatlands. We tested the correlation of median July soil moisture across
181 measurement sites between values calculated either with 1) the ‘universal’ conversion functions
182 or 2) the soil type specific conversion functions, and we found that the Spearman correlation
183 coefficient was as high as 0.98. The difference between these two conversion approaches is in
184 the absolute VWC% values. However, as the conversion did not greatly affect the relative order
185 across the measurement sites, we decided to use the ‘universal’ conversion function for all sites
186 because it produces a much more plausible range of VWC% values.

187 Prior to the conversion, we removed all data where the raw soil moisture count was $<$
188 200, as these counts are far outside the range and indicate that either the given sensor or its
189 installation did not function properly (e.g., sensor was damaged or installed for instance into
190 soils with air pockets). Next, we plotted all individual soil moisture time series month by month

191 and inspected them visually. We identified all days when the data was clearly erroneous (e.g.,
192 times when the sensor was not in the soil or knocked down, for instance, by animals) and
193 removed these days from the rest of the analyses. We also filtered out all soil moisture
194 measurements of periods when the local soil temperature was below 1°C (measured with the
195 same logger at the depth of 6.5 cm), because soil moisture values from frozen soils are invalid
196 (Wild et al., 2019). In addition, we considered and tested additional quality checks, e.g., to
197 identify sudden but soon reversed drops in soil moisture, but after a careful inspection we
198 concluded that the previous check-ups had already removed all suspicious data. For the analyses,
199 we included only sensors with at least 90 % temporal coverage (after the data cleaning explained
200 above) during the measurement period calculated from the melting date (which varies from site
201 to site; Figure 2) until the end of September.

202 2.4 Topographic data

203 We used seven topography variables to explain the soil moisture patterns. These variables
204 were calculated from a high-resolution digital elevation model (DEM). Geographic coordinates
205 were recorded in the field using a high-accuracy Global Navigation Satellite System
206 (GeoExplorer GeoXH 6000 Series; Trimble Inc., Sunnyvale, CA, USA) that provides
207 centimetre-scale positioning accuracy under sufficient (clear-sky) conditions. The high accuracy
208 of the measurement site locations enabled us to relate the soil moisture data with the DEM and
209 its derivatives. The DEM was provided by the National Land Survey of Finland at 2-m resolution
210 (see terrain maps in Figure 1) and was based on Light Detection and Ranging (LiDAR) data
211 covering entire Finland. A similar DEM product and its derivatives were not available for
212 Rásttigáisá study area located in Norway, thus, we decided to exclude Rásttigáisá from the
213 topographic analyses to ensure full comparability of the models.

214 We calculated a topographic wetness index (SAGA wetness index; hereafter SWI)
215 (Conrad et al., 2015) using the Saga Wetness Index tool in the SAGA GIS software (version
216 7.6.2). SWI is a multiple-flow-direction algorithm, which performs well as a proxy for soil
217 moisture compared to other topographic wetness indices (Kopecký et al. 2021; Riihimäki et al.
218 2021). We used the DEM at its finest resolution of 2 m, which performs well when calculating
219 topographical wetness indices (Riihimäki et al. 2021, however, see also Sorensen & Seibert
220 2007; Ågren et al. 2014). We used a filled DEM (following Wang & Liu 2006), and 10 as the
221 suction parameter (t) in calculating SWI.

222 We used a readily-available TWI product at 16-m resolution provided by the Natural
223 Resources Institute Finland (Salmivaara 2016). This TWI product is based on the algorithm by
224 Beven and Kirkby (1979) and includes several improving pre-processing steps, such as the
225 removal of the effect of roads blocking waterflow in the TWI calculations. The flow direction
226 and flow accumulation rasters were calculated with the D_{∞} method (Tarboton 1997).

227 We used a readily-available Cartographic depth-to-water index (DTW; Murphy et al.
228 2009; Ågren et al. 2014) product at 2-m resolution provided by the Natural Resources Institute of
229 Finland (Salmivaara 2020). This DTW product was based on the same DEM that we used in the
230 SWI calculations. DTW was available with stream networks created based on various thresholds
231 from 0.5 to 10 ha. After preliminary tests with the soil moisture data, we decided to use the DTW
232 based on 0.5 ha threshold.

233 We calculated topographic position indices (TPI) in SAGA-GIS software with two radii:
234 20 m and 500 m (hereafter, TPI20 and TPI500). TPI is the relative elevational difference
235 between the focal cell and the mean of its neighbours with a selected radius. Therefore, negative

236 TPI values indicate a hollow and positive a hill or a ridge. Values close zero indicate even terrain
237 or smooth slope.

238 We calculated the potential incoming solar radiation (hereafter, solar radiation) for the
239 summer months (June, July, and August) to reflect the potential energy differences in surface
240 energy balance between different locations. We used the same DEM as in previous calculations
241 and conducted the calculations with the Potential Incoming Solar Radiation tool (Hengl & Reuter
242 2008) in SAGA-GIS software. Solar radiation was first calculated monthly for the midmost days
243 of each month with one-hour intervals, and then, the three summer months were summed
244 together. In the SAGA-GIS software, the algorithm takes into account the shadowing effect of
245 the surrounding terrain as we calculated the visible sky (i.e., sky view factor) using a 10-km
246 search radius and eight looking sectors and included this as an input in the solar radiation
247 function alongside the DEM.

248 Lastly, we calculated a slope-penalized distance to the nearest waterbody index
249 (hereafter, distance to water). Here, we utilized all water features present in the Topographic
250 database of Finland and the DEM provided by National Land Survey of Finland. We calculated
251 the horizontal distance to the nearest water feature with the Accumulated Cost tool in SAGA-
252 GIS software, and we set the slope as the cost surface in the calculations. We considered that the
253 effect of the waterbody reaches further when the slope is even and decreases rapidly when slope
254 is steep. We also considered that the effect of surface waters on soil moisture decreases rather
255 rapidly as the distance increases between a water body and a measurement site. Consequently,
256 we set all cost distance values > 100 to 100. Then, we reversed the index so that index value 100
257 was given to 1) pixels which touch a water body and 2) pixels with zero slope and which are

258 close to a water body. Conversely, index value 0 was given to pixels further away from water
259 bodies over slopy terrain.

260 2.5 Soil data

261 At each measurement point ($n = 503$), we measured organic layer depth and determined
262 soil texture in the field. We determined the main soil type visually and by examining the soil
263 between our fingers, and roughly classified the soils into five soil type categories, namely, clay,
264 silt, sand, gravel, and organic soil (peat). We measured the depth using a thin metal rod (max. 80
265 cm). With the rod, we measured layers 0-10 cm to the nearest centimetre, and for layers > 10 cm,
266 we rounded the measurements to the nearest 5 cm.

267 2.6 Summary statistics of soil moisture variation

268 First, we characterised soil moisture and its variation in each study area by calculating
269 mean soil moisture over all measurement sites and over the measurement period. We calculated
270 average standard deviation both in time (over time within sensors in a given area) and space
271 (over sensors in a given area). Furthermore, we explored how stable the spatial pattern of soil
272 moisture was in the seven study areas by calculating Pearson correlation coefficient between all
273 possible pairs of dates within the measurement period (Kachanoski & de Jong 1988). All
274 statistics were calculated on daily-aggregated (daily medians) soil moisture values.

275 Next, we explored how soil moisture mean was related to soil moisture variation
276 following the methods in Brocca et al. (2012). Here, we calculated soil moisture mean over the
277 measurement sites separately for each measurement date. Respectively, we calculated standard
278 deviation (SD) and coefficient of variation (CV) over measurement sites in each date. We did
279 this for all study areas together and separately for each study area. Then, we inspected 1) how the

280 mean and SD are related (hereafter, mean-SD relationship), and 2) how the mean and CV are
281 related (mean-CV relationship), and here, we applied univariate linear regression models with
282 either linear or quadratic terms. We tested the strength of the nonlinearity in the relationships by
283 comparing the fits of the linear and polynomial models with the ANOVA. If the resulting p-value
284 from ANOVA was sufficiently low (≤ 0.05) for the polynomial predictor, we deemed the
285 relationship as nonlinear.

286 2.7 Statistical models

287 We comprised three sets of models to analyse the influence of topography on spatial soil
288 moisture patterns and its variability in time and across the study areas. We aggregated the soil
289 moisture values into weekly averages for the modelling. We considered only weeks when at least
290 66% of the study sites within a study area had full coverage of soil moisture data (i.e., excluding
291 early spring when majority of the sites in a given area are still under snow).

292 Firstly, we tested how the SWI, TWI, and DTW predicted the weekly mean soil moisture
293 values in univariate linear models (Equations 1-3, Supplementary Figure S1-S3). We chose these
294 three predictors as the focus of the univariate analyses, as they are commonly used proxies for
295 soil moisture (Ågren et al. 2014; Kopecký et al. 2021; Riihimäki et al. 2021). We fitted the linear
296 models in R (version 4.2.1; R Core Team 2022) separately for each study area and week. We
297 treated the weekly mean soil moisture as a response variable, and each of the three topography
298 variables as an explanatory variable one at a time. We tested the predictive accuracy of the
299 models with leave-one-out cross validation (LOOCV), in which each of the measurement sites
300 were one by one removed from the data, rest of the sites used to fit the model. Finally, this model
301 was used to predict soil moisture for the removed measurement sites. After all the measurement

302 sites were predicted ones, these values were compared with the observed values by calculating a
303 squared Spearman correlation coefficient (R^2).

304 Equation 1.

305 *Soil moisture ~ SAGA wetness index*

306 Equation 2.

307 *Soil moisture ~ Topographic wetness index*

308 Equation 3.

309 *Soil moisture ~ Depth to water*

310 Secondly, we fitted linear models (LM) and generalized additive models (GAM) with six
311 topography variables as predictors, namely, TWI, DTW, solar radiation, TPI20, TPI500, and
312 distance to water, and one soil variable, namely, soil type as a categorical predictor (Equation 4;
313 Supplementary Table S2). The number of observations within soil types was highly unbalanced
314 (e.g., very few measurement sites with clay as the main soil type). Thus, we aggregated the soil
315 types into three categories, namely fine soil (including silt and clay), coarse soil (sand and
316 gravel), and organic soil (peat). The soil type predictor represents the effect of soil structure on
317 for instance water infiltration, but it may also the predicted soil moisture levels via controlling
318 for the potential effect of the conversion from raw sensor data into VWC% values. Unlike LM,
319 GAM allows non-linearity in responses. We fitted the GAMs with the restricted maximum
320 likelihood estimation (REML), and to avoid overfitting, we set the maximum dimension of the
321 basis used to represent the smooth term as three. GAMs were fitted with the *mgcv* R package
322 (Wood 2011). Here, we tested how the influence of these predictors on weekly mean soil
323 moisture patterns vary during the measurement period and across the study areas. SWI was

324 excluded from these multiple regressions due to the high correlation between SWI and TWI.
 325 Compared to the SWI algorithm, the TWI algorithm is more commonly used, and the ready TWI
 326 product is openly available for entire Finland. The predictive accuracy of the models was tested
 327 with LOOCV R^2 and root mean squared error (RMSE). We calculated a permutation-based
 328 variable importance metric with the *vi_permute* function from vip package (Greenwell &
 329 Boehmke 2020) to evaluate the relative importance of the predictors. To calculate the variable
 330 importance score, we compared the model fit (R^2) of a model fitted with the original dataset to a
 331 model in which, one at the time, each predictor was randomly permuted; if the permuted
 332 predictor is important, the R^2 will decrease greatly leading into a high importance value. The
 333 variable importance was calculated with 10 permutation rounds per predictor and study area. The
 334 method is model agnostic, and thus, can be compared across different modelling methods
 335 (Greenwell & Boehmke 2020).

336 Equation 4.

$$\begin{aligned}
 337 \quad & \textit{Soil moisture} \sim \textit{Topographic wetness index} + \textit{Depth to water} \\
 338 \quad & \quad + \textit{Topographic position index (500 m radius)} \\
 339 \quad & \quad + \textit{Topographic position index (20 m radius)} + \textit{Soil type} \\
 340 \quad & \quad + \textit{Distace to water} + \textit{Solar radiation}
 \end{aligned}$$

341 Thirdly, we tested if the predictive performance of the multiple regression models was
 342 related to the overall wetness of the study areas. Here, we calculated the Pearson correlation
 343 coefficient between the weekly mean soil moisture and the R^2 value of the corresponding weekly
 344 models. We did this separately for each study area and modelling method. Next, we combined all
 345 these information into a single linear mixed effect model where we explained the R^2 value of the
 346 models by the weekly mean soil moisture. In the model, we included the modelling method (i.e.,

347 LM, GAM) as a categorical predictor and study area as random intercept (Equation 5). We fitted
348 the model by using *lme* function from *nlme* R package (Pinheiro et al. 2022). We evaluated the
349 significance of the relationships by using the F-test from *anova* function.

350 Equation 5.

$$351 \quad R^2 \sim \text{Mean soil moisture} + \text{Modelling method} + (1|\text{Study area})$$

352 Finally, we tested how well the LM and GAM models fitted with the data from one study
353 area predicted the soil moisture values of other study areas. Again, we used R^2 as a measure of
354 predictive power. Here too, we used the mean weekly soil moisture as a predictive variable and
355 the six topography variables as explanatory variables, but tested the model transferability only on
356 weeks, in which the data from both the model fitting and prediction areas had at least 66% soil
357 moisture data coverage. We tested the model transferability only across the study areas, and not
358 in time (i.e., we did not test how model fitted for data from May performed when predicted to
359 data from August, for example).

360 **3 Results**

361 Soil moisture showed large spatial variation but often less pronounced temporal
362 variations across the measurement sites within the seven study areas (Figure 1, Figure 2, Figure
363 3, Table 2). Measurement sites close to each other did not necessarily have similar mean soil
364 moisture values (Figure 1). The soil moisture varied c. 0-60 VWC% at all study areas (Figure 1
365 & 2E). There were both slight drying and wetting trends in the study areas during the study
366 period (Figure 2A & 2C). However, the spatial pattern remained relatively stable thorough the
367 measurement period as the study areas showed high temporal stability (Table 2).

368 On average, there was more spatial variation within the study areas (10.9 - 16.7, standard
 369 deviation across measurement sites) than temporal variation (2.9 - 6.4, standard deviation within
 370 measurement sites) in soil moisture (Table 2). If the study areas were arranged by the average
 371 temporal variation within the areas, the study areas were nearly in their latitudinal order:
 372 northernmost site, Rásttigáisá (tundra), had on average the least amount of temporal variation,
 373 whereas the southernmost site, Karkali (hemiboreal), had the most (Table 2). The amount of
 374 spatial variation in soil moisture within the study areas remained relatively stable during the
 375 measurement period.

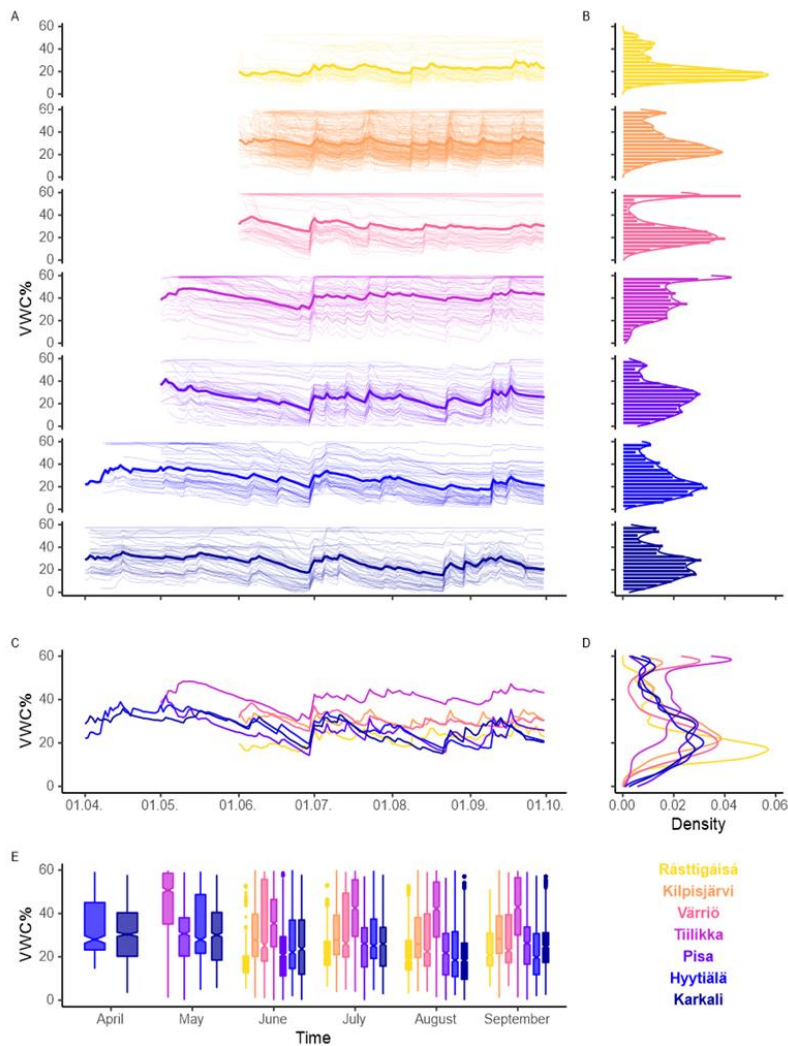
376 Table 2. Soil moisture at the study areas.

Study area	Mean soil moisture (VWC%)	Average temporal variation (Standard deviation)	Average spatial heterogeneity (Standard deviation)	Temporal stability (mean [min, max] spatial correlation)
Rásttigáisá	23.6	2.90	10.9	0.95 [0.71, 1.00]
Kilpisjärvi	30.7	4.67	13.0	0.85 [0.62, 1.00]
Värriö	30.0	4.21	16.7	0.94 [0.72, 1.00]
Tiilikka	41.1	4.74	14.7	0.95 [0.68, 1.00]
Pisa	24.9	5.10	13.7	0.93 [0.75, 1.00]
Hyytiälä	26.9	6.32	13.8	0.90 [0.73, 1.00]
Karkali	26.8	6.35	13.5	0.86 [0.47, 1.00]

377

378 The spatial soil moisture mean-SD soil relationships varied considerably across study
 379 areas (Figure 3A). We found little evidence for a unimodal mean-SD relation relationship since
 380 only one study area (Tiilikka) showed a significant unimodal relationship. However, when
 381 forcing the intercept of the models to zero (as in Brocca et al. 2012), the unimodal relationship

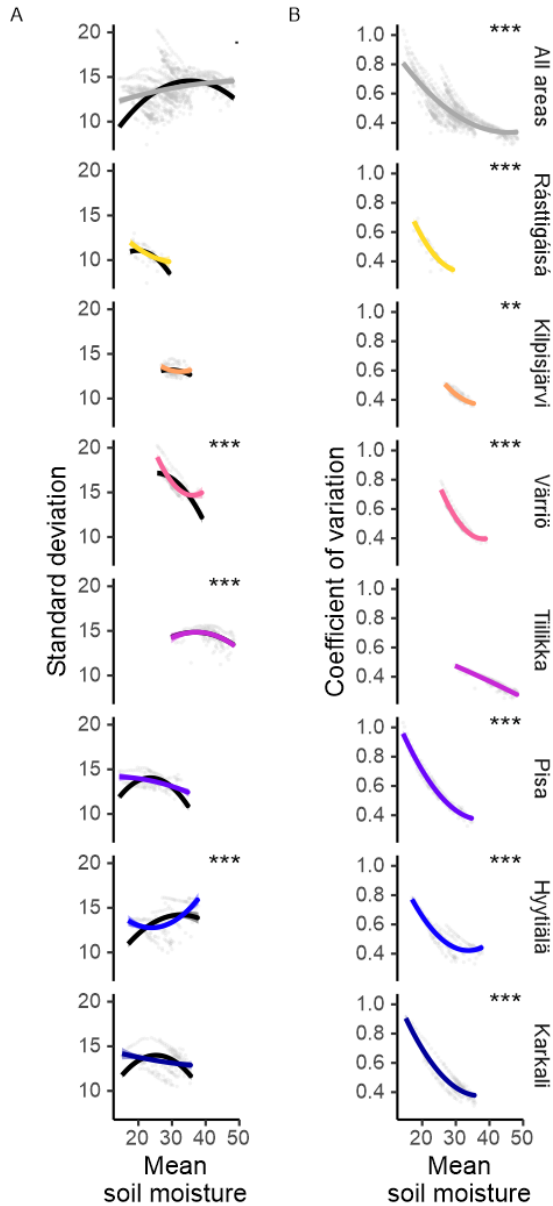
382 was present. The mean-CV relationships followed the same non-linear relationship in all areas
 383 (except Tiilikka) where a decreasing trend levels out towards a minimum CV.



384

385 Figure 2. Temporal variation in soil moisture. The thin lines represent daily mean soil
 386 moisture at the measurement sites (A). The thick lines represent the mean of the areas (A), and
 387 the lines are also presented in relation to each other in (C). The histograms are overlaid with
 388 density plots (B), and the density plots are also presented in relation to each other in (D). The
 389 boxplots represent temporal variation in soil moisture within each area (E). In the box plots, the

390 notches and hinges represent the 25th, 50th, and 75th percentiles, the whiskers represent the 95%
 391 percentile intervals, and the points represent the outliers. VWC%, volumetric water content.



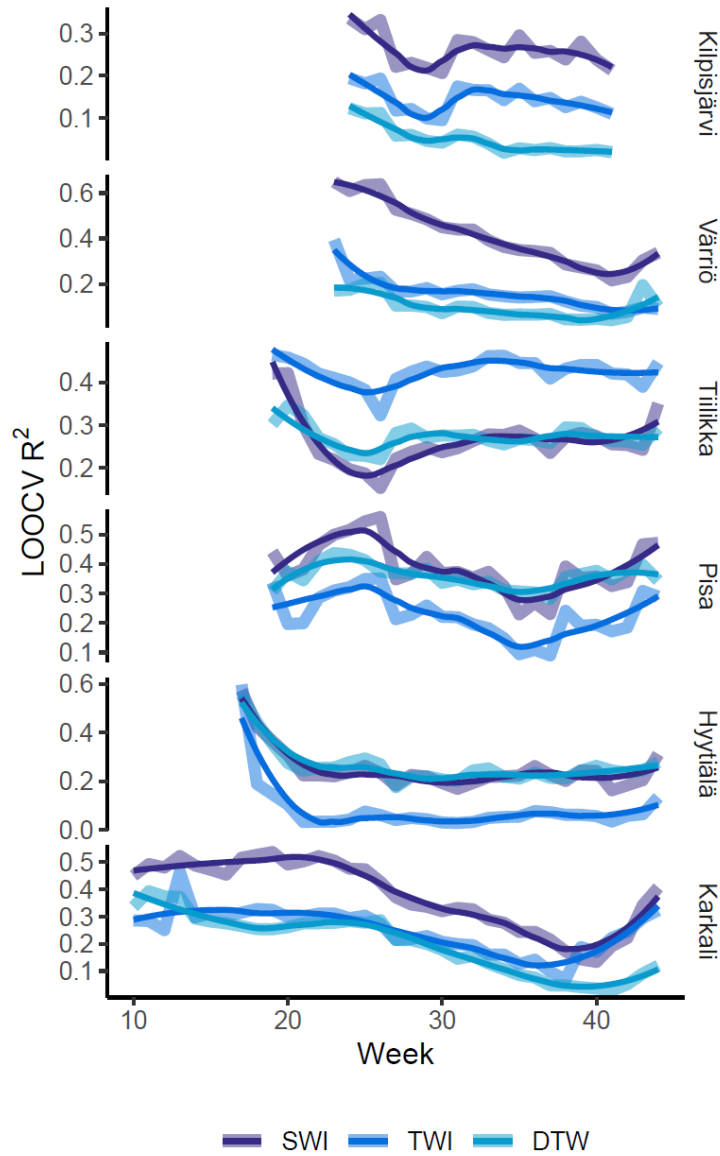
392

393 Figure 3. Soil moisture mean-standard deviation (mean-SD) and mean-coefficient of
 394 variation (mean-CV) relationships. In A), the coloured lines represent the entirely data-driven
 395 quadratic mean-SD relationship, and the black lines represent relationships where the curve is
 396 forced to intersect the y-axis at 0. In B), the coloured lines represent the mean-CV relationship of

397 the areas. The grey dots in the background represent the individual data points, i.e., each dot
398 represent one measurement date. Statistically significant non-linear relationships are marked as
399 follows: ***, p-value ≤ 0.001 ; **, p-value ≤ 0.01 ; ., p-value ≤ 0.1 .

400

401



402

403

404

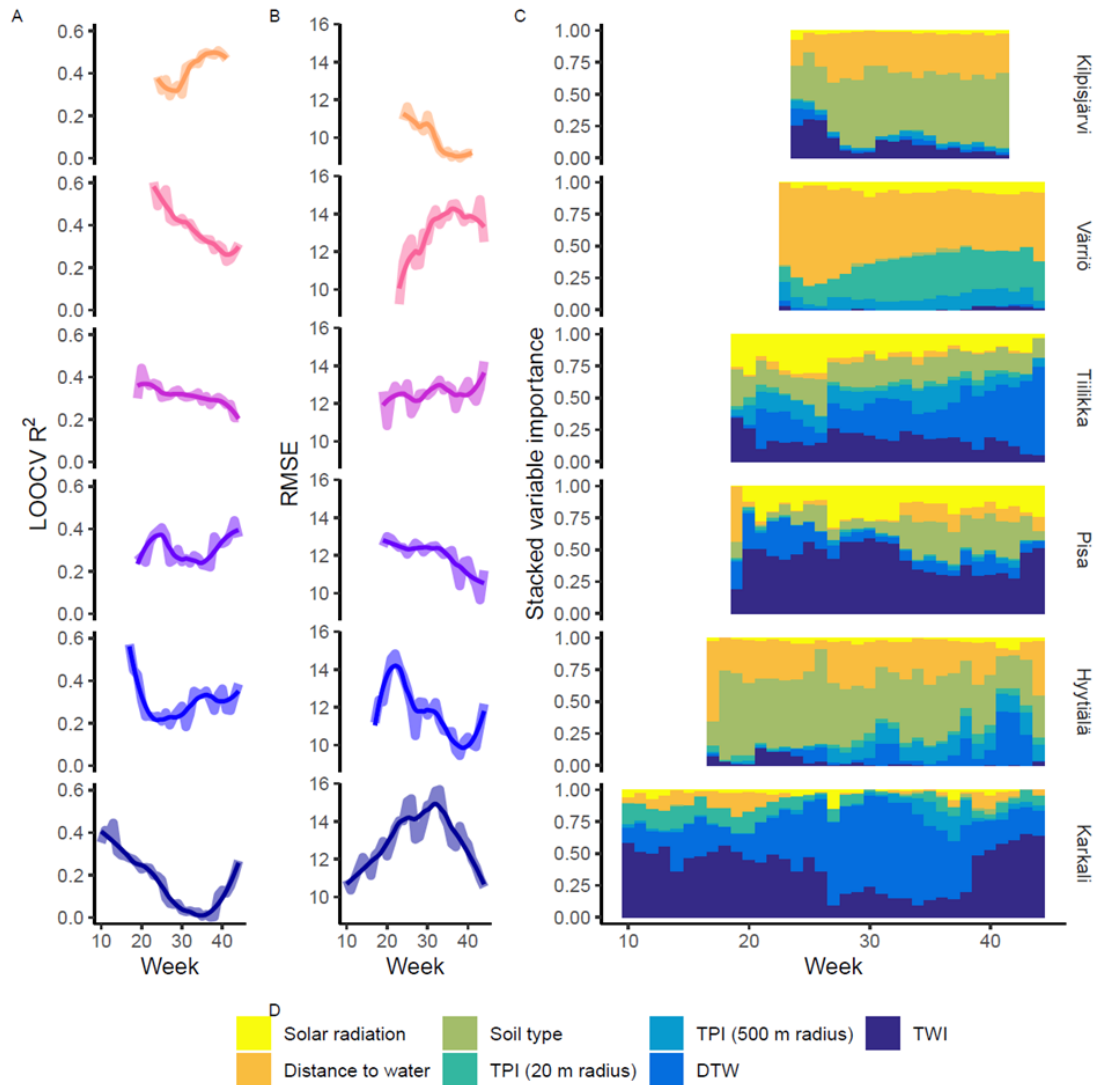
405

406

407

408

Figure 4. Predictive performance of univariate linear models. The lines represent the leave-one-out cross-validated (LOOCV) R^2 results of linear model fitted separately for each week and study area. The colours represent different predictors, namely the SAGA wetness index (SWI), topographic wetness index (TWI), and depth to water (DTW). The thick lines represent the weekly results and the thin lines the smoothed trends (loess smoothing). Maps of the three predictors are provided in Supplementary Figures S1-3.



409

410 Figure 5. Modelling results from generalized additive models (GAM) with six
 411 topography and one soil predictors. The lines represent the predictive performance of the weekly
 412 models as A) the leave-one-out cross-validated (LOOCV) R^2 , and B) LOOCV root-mean-square-
 413 error (RMSE). The thick lines represent the weekly results and the thin line the smoothed trends.
 414 In C), the bars represent stacked variable importance of the predictors in the weekly GAM
 415 models. TPI, topographic position index. DTW, depth to water. TWI, topographic wetness index.
 416 Summary statistics of the predictors are provided in Supplementary Table S2.

417 Modelling results showed that the soil moisture-topography relationships vary in time
418 and across study areas. Weekly linear univariate models (Figure 4) showed that SWI had the
419 highest overall predictive accuracy (averaged LOOCV R^2 over weekly models) in four of the
420 study areas (Kilpisjärvi, mean $R^2 = 0.26$; Värriö, 0.41; Pisa, 0.39; Karkali, 0.38), TWI performed
421 best in one area (Tiilikka, 0.43) and DTW in one area (Hyytiälä 0.26). DTW had typically the
422 lowest predictive performance but the relative order of the three topographic varied and in some
423 study areas (Pisa and Hyytiälä) in some individual weeks DTW scored the highest predictive
424 performance. Also, the slope parameter estimates from the models varied greatly across study
425 areas and also across weeks (Supplementary Figure S4).

426 Predictive performance of the multiple regression models showed similar pattern in space
427 and time compared to the best performing univariate LM (GAM results in Figure 5A and 5B,
428 LM results in Supplementary Figure S5A and S5B). Overall predictive performance was highest
429 in models for Kilpisjärvi (mean LOOCV R^2 over weekly models and modelling methods = 0.42)
430 followed by Värriö (0.39), Hyytiälä (0.33), Pisa (0.31), Tiilikka (0.30), and Karkali (0.18). The
431 predictive performance was on average slightly higher for LM (0.31) than GAM (0.30), but the
432 difference was not significant (paired Wilcoxon signed rank test, $p = 0.53$). On average, LOOCV
433 RMSE was 11.8 for LM and 12.2 for GAM, and the difference was significant ($p = 0.018$). The
434 variable importance scores also varied across weeks for some areas (e.g., Karkali), while in
435 others, the scores remained relatively stable (e.g., Pisa) (Figure 5C). On average, the most
436 important variable for predicting soil moisture was TWI in three of the study areas (Tiilikka,
437 Pisa, and Karkali), soil type in two areas (Kilpisjärvi and Hyytiälä) and the slope penalized
438 distance to waterbodies in one area (Värriö). Variable importance scores for the topographic

439 predictors followed similar patterns in GAM (Figure 5C) and LM (Supplementary Figure S5C),
440 but the scores varied greatly from area to another.

441 The predictive performance of the multiple regression model was weakly, positively
442 related to the overall wetness of the soils in the study areas (Supplementary Table S3).
443 Correlation coefficient was positive in 9 out of 12 occasions (modelling methods \times study areas)
444 but only three positive correlations were significant ($p \leq 0.05$) and none of the negative
445 relationships were significant. The GAM models for Karkali showed the highest correlation
446 coefficient (0.74, $p < 0.001$), and the LM models for Kilpisjärvi the lowest (-0.31, $p = 0.20$).
447 However, a mixed effect model which combined both modelling methods and all study areas,
448 indicated a positive and significant (F-test, $p > 0.001$) relationship between the mean soil
449 moisture and LOOCV R^2 .

450 Lastly, we tested how well the multiple regression models fitted in one study area
451 performed when predicting soil moisture values of other areas (Supplementary Figure S6 & S7).
452 LMs had better model transferability on average (LOOCV $R^2 = 0.23$; LOOCV RMSE = 17.2)
453 than GAMs (0.19; 19.6), and the difference was also significant ($p < 0.001$ in R^2 and $p = 0.031$ in
454 RMSE). Models fitted with data from Kilpisjärvi ($R^2 = 0.33$; RMSE = 14.6) and Pisa (0.27; 14.0)
455 performed best on average when these models were used for predicting soil moisture in other
456 areas. Whereas models fitted with data from Hyytiälä (0.12; 20.2) and Tiilikka (0.16; 31.2) had
457 low performance predicting soil moisture in other areas.

458 **4 Discussion**

459 4.1 Soil moisture in boreal forest and tundra environments

460 This study design and data recorded over several months revealed the locally
461 heterogeneous patterns of soil moisture across and within boreal forest and tundra environments.
462 Our results highlight that wide soil moisture gradients are present at small spatial extents, and
463 that similar soil moisture gradients (0-60 VWC%) can be found locally from the tundra of
464 northern Norway to the hemiboreal forests of southern Finland. Here, we also showed that soil
465 moisture is relatively stable over time in the majority of the measurement sites ($n = 503$), and
466 that across these environments, the spatial soil moisture pattern remains similar through the
467 measurement period (April-September).

468 We found that there were also some measurement sites where soil moisture varied
469 considerably in time. Studying these anomalous sites and their environmental conditions and
470 ecosystem processes in more detail could be one important target for future studies to understand
471 why and how they are different from the landscape matrices. Furthermore, if the annual
472 precipitation increases but heat waves intensify in the northern environments due to climate
473 change, the patterns of soil moisture variation can be very different in the upcoming decades
474 (Samaniego et al., 2018). Thus, it is important to investigate if the heterogeneous soil moisture
475 regimes can provide a buffer for ecosystems against increasing temperatures in the boreal forest
476 and tundra environments. Overall, there is a need for comprehensive study designs that monitor
477 soil moisture across distinct environments and over large spatial and temporal extents (Dorigo et
478 al. 2021).

479 4.2 General patterns of soil moisture variation

480 In general, the mean-SD relationship follows a unimodal pattern, in which sites with high
481 and low mean soil moisture values express less variation compared to sites with intermediate
482 mean soil moisture values (Pan & Peters-Lidard, 2008; Scaife et al., 2021). However here, we
483 found only a weak signal of this unimodal mean-SD relationship. This is likely due to the
484 temporal stability of soil moisture in the seven study areas. Overall, we found less temporal
485 variation in mean soil moisture of the seven study areas in comparison to other studies (see e.g.,
486 Penna et al. 2009; Brocca et al. 2012; Rosenbaum et al. 2012; Dymond et al. 2021). Lawrence &
487 Hornberg (2007) concluded that in humid regions, soil moisture variance decreases when mean
488 soil moisture increases, and that in temperate regions, variance peaks at intermediate soil
489 moisture contents. During the measurement period from April to September, we did not find
490 extreme drying or wetting in the study areas. Therefore, the data do not cover situations where
491 the very high or very low soil moisture values would force the mean-SD relationship into lower
492 SD values in either ends of the mean soil moisture gradient. Thus, our findings are somewhat
493 analogous with findings by Martínez-Fernández & Ceballos (2003). They found a monotonously
494 increasing relationship between mean soil moisture and variance, but they found that mean soil
495 moisture was always rather low, and thus, it likely covered only part of the whole potential soil
496 moisture gradient.

497 We found a similar mean-CV relationship as in previous investigations (see e.g.,
498 Famiglietti et al. 2008; Penna et al. 2009; Brocca et al. 2012): a decreasing trend that eventually
499 levels. Although, in comparison to previous investigations conducted in different ecosystems, we
500 found much higher spatial variability across all measurement dates and thus across all mean soil
501 moisture levels present in our data. Overall, we found that the spatial patterns remained relatively

502 stable over time, and thus, these seven study areas are likely less prone to large temporal
503 variation in standard deviation across measurement sites. This is also in line with previous
504 investigations, which have shown that in tundra environments, the spatial patterns of soil
505 moisture are relatively stable during growing season (le Roux et al. 2013; Kemppinen et al.
506 2018; Tyystjärvi et al. 2021).

507 4.3 Soil moisture-topography relationships

508 Soil moisture-topography relationships turned out to be context-dependent. This was
509 expected, because of the other factors (e.g., vegetation, local temperatures) that control soil
510 moisture and interact with topography. Thus, no single topography-based variable can manifest
511 these relationships in all the study areas and conditions. We found that topography-based proxies
512 cannot predict soil moisture patterns with over the entire measurement period and across seven
513 distinct study areas. This is important because topography-based proxies are widely used instead
514 of field-quantified soil moisture in climate change and biodiversity modelling (Kopecký et al.
515 2021; Riihimäki et al. 2021), although topography is only one of the drivers of soil moisture
516 patterns (Albertson & Montaldo, 2003; Teuling, 2005; Wilson et al., 2004). Our results
517 demonstrate why topography-based proxies for soil moisture should not be used without
518 exhaustive investigations on their capability to characterise soil moisture patterns over space and
519 time. This is especially important to consider in studies with large spatial extents and where high
520 model transferability is required. By neglecting these investigations, topography-based proxies
521 can lead to biased inferences on the importance of soil moisture, for instance, in ecological
522 models (Kopecký & Čížková 2010). Overall, we encourage careful consideration whenever soil
523 moisture data are substituted with topography-based proxies (Kopecký et al. 2021; Riihimäki et

524 al. 2021) or optical proxies (von Oppen et al. 2021), regardless if soil moisture is modelled with
525 statistical (Kemppinen et al. 2018) or process-based methods (Tyystjärvi et al. 2021).

526 Here, we showed that the influence of topography on soil moisture varies from study area
527 and week to another. This means that, for instance, TWI is likely to perform well in
528 heterogenous forest terrains (Tiilikka, Pisa) throughout the measurement period. Whereas in
529 mountain tundra terrains (Kilpisjärvi), TWI tends to perform well only immediately after
530 snowmelt when the landscape is very wet, and at other times, soil type was the most important
531 predictor. This is in line with previous research which have reported temporal variation in the
532 performance of topography as a proxy for field-quantified soil moisture (Western et al. 1999;
533 Tague et al. 2010; Ali et al. 2014; Riihimäki et al. 2021), and here, we showed this with a
534 harmonized study design across large geographic distances characterised by various
535 environmental conditions, and for the entire snowless season of the boreal forest and tundra
536 environments.

537 Our analyses did not show particularly clear trends in the strength of the soil moisture-
538 topography relationships during the measurement period shared by all study areas, but there was
539 a slight tendency that the topographic models had higher predictive accuracy early on the
540 snowless season (i.e., after snowmelt) than later in the season. In the sub-Arctic tundra,
541 Riihimäki et al. (2021) also found that various TWI algorithms had stronger links to early season
542 soil moisture (i.e., after snowmelt) than to the late season soil moisture. In other environments,
543 the temporal variation of the soil moisture-TWI relationship has been linked to the overall
544 wetness of the landscape (i.e., precipitation) (Western et al. 1999; Ali et al. 2014), and we too
545 found that the model performance was slightly higher when the mean soil moisture across
546 measurement sites was higher. Also, the temporal variation (or temporal instability) of the

547 relationship is dependent on soil and vegetation factors (Coleman & Niemann 2013). Our results
548 together with previous literature imply that in seasonally snow-covered environments,
549 topography has stronger control on soil moisture shortly after snowmelt, and that the soil
550 moisture-topography relationship weakens towards the end of the snowless season when other
551 factors (e.g., evaporation, transpiration) play a greater role in controlling soil moisture patterns.

552 We found no single topography variable superior to others in predicting soil moisture
553 patterns across all study areas, as the most influential predictors varied from area to another, and
554 to some extent, also from week to week. For instance, in Karkali, the most relevant predictor
555 changed from week after week, whereas in Pisa, one predictor (TWI) remained the most relevant
556 for most of the measurement period. Furthermore, the transferability of the topographic models
557 from one area to another varied. The models that were fitted with data from the study areas
558 mostly covered by peatlands (Hyytiälä and Tiilikka) performed very poorly when they were used
559 for predicting soil moisture in other areas. This indicates that soil moisture-topography
560 relationships in wetland areas can be very different from other environments. Overall, our results
561 highlight the need for detailed exploration and careful consideration of different topography
562 variables in various environmental settings before applying them as proxies for soil moisture.

563 4.4 Challenges in measuring soil moisture

564 Methodological challenges are various in soil moisture research, particularly related to
565 field measurements (Robinson et al., 2008). Until recently, devices for continuous data have
566 been expensive, which is impractical for detailed investigations over large spatial and temporal
567 extents (Wild et al., 2019). Also, there are numerous device types that are based on different
568 measurement techniques (Dobriyal et al., 2012; Romano, 2014; Yu et al., 2021). Moreover,
569 different device types based on the same technique can provide significantly different results

570 (Lekshmi et al., 2014; Walker et al., 2004), even the same device type can provide different
571 values (Rosenbaum et al. 2010). In this study, we used only one device type to reduce
572 uncertainty caused by different instruments (Wild et al., 2019), yet the manufacturer of the
573 devices reports that error among the devices can be up to 5%. This is due to differences between
574 the devices and soil types, and it cannot be controlled for, at least at the present moment. Soil
575 type also influences the conversion of raw moisture measurements into volumetric water content.
576 Here, we used a single conversion function adopted from Kopecký et al. (2021) as the previous
577 functions (Wild et al., 2019) were created for different soils in the Czech Republic, and were
578 considered difficult to apply for these northern study areas (typically high content of organic soil
579 material) based on our preliminary tests (data not shown). As this specific sensor type is
580 becoming more common among scientists across different ecosystems and soil types, we identify
581 this as an important subject for development in the near future. Yet, at the same time, we
582 consider that the data conversion is not a major issue in our study where the moisture gradient is
583 wide and differences across measurement sites are considerable. Thus, with these approaches we
584 managed to tackle critical challenges related to soil moisture measurements (Robinson et al.,
585 2008).

586 4.5 Future perspectives

587 One of main challenges remains for better understanding and modelling of spatio-
588 temporal patterns of soil moisture and its effects on ecosystems: How to obtain field-quantified
589 data on fine-scale patterns of soil moisture and its controlling factors with sufficient accuracy
590 and extensive spatio-temporal coverage? Here, we found high temporal stability in soil moisture
591 and its spatial patterns in boreal forests and the tundra of northern Europe, from peatlands to
592 mountain tops. However, for instance in the tundra, soil moisture often varies greatly from one

593 square meter to another (Kemppinen et al. 2019, 2021a). Consequently, further applications,
594 such as ecological and biogeographical investigations, would require soil moisture data at a
595 corresponding spatial resolution, and this is challenging regardless of methodology (e.g.,
596 statistical or process-based modelling). Here, we addressed the influence of fine-scale
597 topography and soil properties on soil moisture, and the next step would be to incorporate the
598 influence of fine-scale vegetation and local temperatures. Therefore, more data and models are
599 needed on fine-scale soil moisture and its controlling factors, and particularly, more temporal
600 data on vegetation and local temperatures. Our soil moisture data covered a single growing
601 season and thus, it is likely that the data did not capture occasional extreme conditions (drought
602 and flooding). Therefore, long-term measurements are needed to capture the full potential range
603 in soil moisture dynamics. Finally, northern Europe is a seasonally snow-covered region, and
604 thus, investigations on soil moisture-snow relationships are urgently needed for understanding
605 the future soil moisture in boreal forest and tundra environments that are under rapid climate
606 change.

607 **5 Conclusions**

608 Here, we present a rare case of intensive soil moisture investigations which cover large
609 geographical and environmental gradients and the entire snowless season of the boreal forest and
610 tundra environments in northern Europe. We documented detailed soil moisture patterns at high
611 temporal resolution in 503 locations within seven study areas from southern Finland to northern
612 Norway. We found that soil moisture has high spatial variability in all seven study areas, and that
613 the variability persisted the entire six-month measurement period. We also found that the nature
614 of soil moisture-topography relationships varied greatly across time and space. Overall, we
615 highlight that wide soil moisture gradients can be present at small spatial extents, and that similar

616 soil moisture gradients can be found locally across northern Europe from hemiboreal forests to
617 the tundra.

618 **Open Research**

619 Data and code are openly available (Kemppinen, 2022). Data and code will be deposited
620 to Zenodo once the manuscript is accepted.

621 **Author contribution**

622 JK and PN conceptualised the research. JK, PN, JA, and ML conceptualised the study
623 setting. PN performed data curation. JK and PN analysed the data. JK, JA, and ML acquired the
624 funding. JK, PN, TR, VT, JA, and ML carried out the field investigations. JK visualised the
625 results. JK and PN wrote the original draft. JK, PN, TR, VT, JA, and ML reviewed and edited
626 the draft.

627 **Acknowledgements**

628 We thank the personnel at the Kilpisjärvi Biological research station, Kevo Subarctic
629 Research Institute, Värriö Subarctic Research Station, and Hyytiälä Forestry Field Station for
630 their support during fieldwork. We acknowledge funding for fieldwork and equipment by the
631 Nordenskiöld samfundet, Tiina and Antti Herlin foundation, and Maa- ja vesitekniikan tuki ry..
632 JK was funded by the Academy of Finland (project number 349606), and the Arctic Interactions
633 at the University of Oulu and Academy of Finland (project number 318930, Profi 4). PN was
634 funded by the Academy of Finland (project number 347558), the Nessling foundation, and the
635 Kone Foundation. TR was funded by the Doctoral Program in Geosciences, University of
636 Helsinki. JA acknowledges the Academy of Finland Flagship funding (project number 337552).

637 **Permissions**

638 Permission to carry out fieldwork was granted by Metsähallitus.

639

640 **References**

641 Aalto, J., H. Riihimäki, E. Meineri, K. Hylander & M. Luoto (2017). Revealing topoclimatic
642 heterogeneity using meteorological station data. *International Journal of Climatology* 37(S1),
643 544-556. <https://doi.org/10.1002/joc.5020>

644

645 Aalto, J., Tyystjärvi, V., Niittynen, P., Kemppinen, J., Rissanen, T., Gregow, H., & Luoto, M.
646 (2022). Microclimate temperature variations from boreal forests to the tundra. *Agricultural and*
647 *Forest Meteorology*.

648

649 Ackerman, D., Griffin, D., Hobbie, S. E., & Finlay, J. C. (2017). Arctic shrub growth trajectories
650 differ across soil moisture levels. *Global Change Biology*, 23(10), 4294–4302.

651

652 Albertson, J. D., & Montaldo, N. (2003). Temporal dynamics of soil moisture variability: 1.
653 Theoretical basis. *Water Resources Research*, 39(10). <https://doi.org/10.1029/2002wr001616>

654

655 Ali, G., Birkel, C., Tetzlaff, D., Soulsby, C., McDonnell, J.J. & Tarolli, P. (2014), A comparison
656 of wetness indices for the prediction of observed connected saturated areas under contrasting
657 conditions. *Earth Surface Processes and Landforms*, 39: 399-413.

658 <https://doi.org/10.1002/esp.3506>

659

- 660 Bartsch, A., Balzter, H., & George, C. (2009). The influence of regional surface soil moisture
661 anomalies on forest fires in Siberia observed from satellites. *Environmental Research Letters:*
662 *ERL [Web Site]*, 4(4), 045021.
- 663
- 664 Beven, K. J., & Kirkby, M. J. (1979). A physically based, variable contributing area model of
665 basin hydrology / Un modèle à base physique de zone d'appel variable de l'hydrologie du bassin
666 versant. *Hydrological Sciences Bulletin*, 24(1), 43–69.
- 667
- 668 Bintanja, R., van der Wiel, K., van der Linden, E. C., Reusen, J., Bogerd, L., Krikken, F., &
669 Selten, F. M. (2020). Strong future increases in Arctic precipitation variability linked to
670 poleward moisture transport. *Science Advances*, 6(7), eaax6869.
- 671
- 672 Bjorkman, A. D., Myers-Smith, I. H., Elmendorf, S. C., Normand, S., Rüger, N., Beck, P. S. A.,
673 Blach-Overgaard, A., Blok, D., Cornelissen, J. H. C., Forbes, B. C., Georges, D., Goetz, S. J.,
674 Guay, K. C., Henry, G. H. R., HilleRisLambers, J., Hollister, R. D., Karger, D. N., Kattge, J.,
675 Manning, P., ... Weiher, E. (2018). Plant functional trait change across a warming tundra biome.
676 *Nature*, 562(7725), 57–62.
- 677
- 678 Brocca, L., Tullo, T., Melone, F., Moramarco, T., & Morbidelli, R. (2012). Catchment scale soil
679 moisture spatial–temporal variability. *Journal of Hydrology*, 422-423, 63-75.
- 680
- 681 Chapin, F. S., 3rd, Mcguire, A. D., Randerson, J., Pielke, R., Baldocchi, D., Hobbie, S. E.,
682 Roulet, N., Eugster, W., Kasischke, E., Rastetter, E. B., Zimov, S. A., & Running, S. W. (2000).

683 Arctic and boreal ecosystems of western North America as components of the climate system.
684 *Global Change Biology*, 6(S1), 211–223.

685
686 Coleman, M. L., and Niemann, J. D. (2013), Controls on topographic dependence and temporal
687 instability in catchment-scale soil moisture patterns, *Water Resources Research*, 49, 1625– 1642,
688 doi:10.1002/wrcr.20159.

689
690 Conrad, O., Bechtel, B., Bock, M., Dietrich, H., Fischer, E., Gerlitz, L., Wehberg, J., Wichmann,
691 V., & Böhner, J. (2015). System for Automated Geoscientific Analyses (SAGA) v. 2.1.4.
692 *Geoscientific Model Development*, 8(7), 1991–2007.

693
694 Crave, A., & Gascuel-Oudou, C. (1997). The influence of topography on time and space
695 distribution of soil surface water content. *Hydrological Processes*, 11(2), 203–210.
696 [https://doi.org/10.1002/\(SICI\)1099-1085\(199702\)11:2<203::AID-HYP432>3.0.CO;2-K](https://doi.org/10.1002/(SICI)1099-1085(199702)11:2<203::AID-HYP432>3.0.CO;2-K)

697
698 Dobriyal, P., Qureshi, A., Badola, R., & Hussain, S. A. (2012). A review of the methods
699 available for estimating soil moisture and its implications for water resource management.
700 *Journal of Hydrology* , 458-459, 110–117.

701
702 D’Orangeville, L., Duchesne, L., Houle, D., Kneeshaw, D., Côté, B., & Pederson, N. (2016).
703 Northeastern North America as a potential refugium for boreal forests in a warming climate.
704 *Science*, 352(6292), 1452–1455.

705

706 Dorigo, W., Himmelbauer, I., Aberer, D., Schremmer, L., Petrakovic, I., Zappa, L.,
707 Preimesberger, W., Xaver, A., Annor, F., Ardö, J., Baldocchi, D., Bitelli, M., Blöschl, G.,
708 Bogena, H., Brocca, L., Calvet, J-C., Camarero, J. J., Capello, G., Choi, M., Cosh, M. C., Van
709 De Giesen, N., Hajdu, I., Ikonen, J., Jensen, K. H., Devi Kanniah, K., De Kat, I., Kirchengast,
710 G., Kumar Rai, P., Kyrouac, J., Larson, K., Liu, S., Loew, A., Moghaddam, M., Martínez
711 Fernández, J., Bader, C. M., Morbidelli, R., Musial, J. P., Osenga, E., Palecki, M. A., Pellarin,
712 T., Petropoulos, G. P., Pfeil, I., Powers, J., Robock, A., Rüdiger, C., Rummel, U., Strobel, M.,
713 Su, Z., Sullivan, R., Tagesson, T., Varlagin, A., Vreugdenhil, M., Walker, J., Wen, J., Wenger,
714 F., Wigneron, J. P., Woods, M., Yang, K., Zeng, Y., Zhang, X., Zreda, M., Dietrich, S., Gruber,
715 A., Van Oevelen, P., Wagner, W., Scipal, K., Drusch, M., & Sabia, R. (2021). The International
716 Soil Moisture Network: serving Earth system science for over a decade, *Hydrol Earth Syst Sc*,
717 25(11), 5749-5804.

718
719 Dymond, S. F., Wagenbrenner, J. W., Keppler, E., T., & Bladon, K. D. Dynamic Hillslope Soil
720 Moisture in a Mediterranean Montane Watershed. *Water Resources Research*, 57: 11.

721
722 Green, J. K., Seneviratne, S. I., Berg, A. M., Findell, K. L., Hagemann, S., Lawrence, D. M., &
723 Gentine, P. (2019). Large influence of soil moisture on long-term terrestrial carbon uptake.
724 *Nature*, 565(7740), 476–479.

725
726 Greenwell, B., & Boehmke, B. C. (2020). *The R Journal* (2020) 12:1, pages 343-366.

727 <https://journal.r-project.org/archive/2020/RJ-2020-013/index.html>

728

729 Famiglietti, J. S., Ryu, D., Berg, A. A., Rodell, M., & Jackson, T. J. (2008). Field observations of
730 soil moisture variability across scales. *Water Resources Research*, 44(1).

731

732 Hattab, T., Garzón-López, C. X., Ewald, M., Skowronek, S., Aerts, R., Horen, H., Brasseur, B.,
733 Gallet-Moron, E., Spicher, F., Decocq, G., Feilhauer, H., Honnay, O., Kempeneers, P.,

734 Schmidtlein, S., Somers, B., Van De Kerchove, R., Rocchini, D., & Lenoir, J. (2017). A unified
735 framework to model the potential and realized distributions of invasive species within the
736 invaded range. *Diversity & Distributions*, 23(7), 806–819.

737

738 Hattab, T., & Lenoir, J. (2017). iSDM: Invasive Species Distribution Modelling. R package
739 version 1.0. <https://CRAN.R-project.org/package=iSDM>

740

741 Hawkes, C. V., Waring, B. G., Rocca, J. D., & Kivlin, S. N. (2017). Historical climate controls
742 soil respiration responses to current soil moisture. *Proceedings of the National Academy of
743 Sciences of the United States of America*, 114(24), 6322–6327.

744

745 Hengl, T., & Reuter, H. I. (Eds.). (2008). *Geomorphometry: concepts, software, applications*.
746 Newnes.

747

748 Hiltbrunner, D., Zimmermann, S., Karbin, S., Hagedorn, F., & Niklaus, P. A. (2012). Increasing
749 soil methane sink along a 120-year afforestation chronosequence is driven by soil moisture.

750 *Global Change Biology*, 18(12), 3664–3671.

751

- 752 Humphrey, V., Berg, A., Ciais, P., Gentine, P., Jung, M., Reichstein, M., Seneviratne, S. I., &
753 Frankenberg, C. (2021). Soil moisture-atmosphere feedback dominates land carbon uptake
754 variability. *Nature*, 592(7852), 65–69.
- 755
- 756 Kachanoski, R. G. & de Jong, E. 1988. Scale dependence and the temporal persistence of spatial
757 patterns of soil water storage. *Water Resources Research*, 24(1):85-91.
- 758
- 759 Kemppinen, J. (2022). soilMoistFennoscandia. [Dataset]
760 <https://github.com/jkemppinen/soilMoistFennoscandia>
- 761
- 762 Kemppinen, J., Niittynen, P., Riihimäki, H., & Luoto, M. (2018). Modelling soil moisture in a
763 high-latitude landscape using LiDAR and soil data. *Earth Surface Processes and Landforms*,
764 43(5), 1019–1031.
- 765
- 766 Kemppinen, J. & Niittynen, P. (2022). Microclimate relationships of intraspecific trait variation
767 in sub-Arctic plants. *Oikos*, e09507.
- 768
- 769 Kemppinen, J., Niittynen, P., Aalto, J., le Roux, P.C., & Luoto, M. (2019). Water as a resource,
770 stress and disturbance shaping tundra vegetation. *Oikos*, 128: 811–822.
- 771
- 772 Kemppinen, J., Niittynen, P., le Roux, P.C., Momberg, M., Happonen, K., Aalto, J., Rautakoski,
773 H., Enquist, B., Vandvik, V., Halbritter, A.H., Maitner, B., & Luoto, M. (2021a). Consistent trait-

774 environment relationships across tundra plant communities. *Nature Ecology and Evolution*, 5,
775 458–467.

776

777 Kopecký, M. & Čížková, S. (2010). Using topographic wetness index in vegetation ecology:
778 does the algorithm matter? *Applied Vegetation Science*, 13(4), 450-459.

779

780 Kopecký, M., Macek, M., & Wild, J. (2021). Topographic Wetness Index calculation guidelines
781 based on measured soil moisture and plant species composition. *The Science of the Total*
782 *Environment*, 757, 143785.

783

784 Koster, R. D., Dirmeyer, P. A., Guo, Z., Bonan, G., Chan, E., Cox, P., Gordon, C. T., Kanae, S.,
785 Kowalczyk, E., Lawrence, D., Liu, P., Lu, C.-H., Malyshev, S., McAvaney, B., Mitchell, K.,
786 Mocko, D., Oki, T., Oleson, K., Pitman, A., ... GLACE Team. (2004). Regions of strong
787 coupling between soil moisture and precipitation. *Science*, 305(5687), 1138–1140.

788

789 Lawrence, J. E., & Hornberger, G. M. (2007). Soil moisture variability across climate zones.
790 *Geophysical Research Letters*, 34(20).

791

792 Lekshmi, S., Singh, D. N., & Shojaei Baghini, M. (2014). A critical review of soil moisture
793 measurement. *Measurement*, 54, 92–105.

794

795 Lowry, C. S., Loheide, S. P., Moore, C. E., & Lundquist, J. D. (2011), Groundwater controls on
796 vegetation composition and patterning in mountain meadows, *Water Resources Research*, 47,
797 W00J11, doi:10.1029/2010WR010086.

798

799 Martínez-Fernández, J., & Ceballos, A. (2003). Temporal stability of soil moisture in a large-
800 field experiment in Spain. *Soil Science Society of America Journal*, 67(6), 1647–1656.

801

802 McColl, K. A., Alemohammad, S. H., Akbar, R., Konings, A. G., Yueh, S., & Entekhabi, D.
803 (2017). The global distribution and dynamics of surface soil moisture. *Nature Geoscience*, 10(2),
804 100–104.

805

806 McLaughlin, B. C., Ackerly, D. D., Klos, P. Z., Natali, J., Dawson, T. E., & Thompson, S. E.
807 (2017). Hydrologic refugia, plants, and climate change. *Global Change Biology*, 23(8), 2941–
808 2961.

809

810 Murphy, P.N.C., Ogilvie, J. and Arp, P. (2009), Topographic modelling of soil moisture
811 conditions: a comparison and verification of two models. *European Journal of Soil Science*, 60:
812 94-109. <https://doi.org/10.1111/j.1365-2389.2008.01094.x>

813

814 Niittynen, P., Heikkinen, R.K. & Luoto, M. (2018). Snow cover is a neglected driver of Arctic
815 biodiversity loss. *Nature Clim Change* 8, 997–1001.

816

817 Oki, T., Entekhabi, D., & Harrold, T. I. (2004). The global water cycle. In *Geophysical*
818 *Monograph Series* (pp. 225–237). American Geophysical Union.

819

820 von Oppen, J., Normand, N., Bjorkman, A. D., Blach-Overgaard, A., Assmann, J. J.,
821 Forchhammer, M., Guéguen, M. & Nabe-Nielsen, J. 2021. Annual air temperature variability and
822 biotic interactions explain tundra shrub species abundance. *Journal of Vegetation Science*, 32(2),
823 e13009.

824

825 Penna, D., Borga, M., Norbiato, D., & Dalla Fontana, G. (2009). Hillslope scale soil moisture
826 variability in a steep alpine terrain. *Journal of Hydrology* , 364(3-4), 311–327.

827

828 Pinheiro J., Bates D., & R Core Team (2022). nlme: Linear and Nonlinear Mixed Effects
829 Models. R package version 3.1-157, <<https://CRAN.R-project.org/package=nlme>>

830

831 Pirinen, P., Simola, H., Aalto, J., Kaukoranta, J. P., Karlsson, P., & Ruuhela, R. (2012).
832 Climatological statistics of Finland 1981–2010. *Finnish Meteorological Institute Reports*, 1, 1-
833 96.

834

835 Post, E., Alley, R. B., Christensen, T. R., Macias-Fauria, M., Forbes, B. C., Gooseff, M. N., Iler,
836 A., Kerby, J. T., Laidre, K. L., Mann, M. E., Olofsson, J., Stroeve, J. C., Ulmer, F., Virginia, R.
837 A., & Wang, M. (2019). The polar regions in a 2°C warmer world. *Science Advances*, 5(12),
838 eaaw9883.

839

840 R Core Team (2022). R: A language and environment for statistical computing. R Foundation for
841 Statistical Computing, Vienna, Austria. <https://www.R-project.org/>

842

843 Rantanen, M., Karpechko, A. Y., Lipponen, A., Nordling, K., Hyvärinen, O., Ruosteenoja, K.,
844 Vihma, T., & Laaksonen, A. (2022). The Arctic has warmed nearly four times faster than the
845 globe since 1979. *Communications Earth & Environment* 3, 168. [https://doi.org/10.1038/s43247-](https://doi.org/10.1038/s43247-022-00498-3)
846 [022-00498-3](https://doi.org/10.1038/s43247-022-00498-3)

847

848 Rasmijn, L. M., van der Schrier, G., Bintanja, R., Barkmeijer, J., Sterl, A., & Hazeleger, W.
849 (2018). Future equivalent of 2010 Russian heatwave intensified by weakening soil moisture
850 constraints. *Nature Climate Change*, 8(5), 381–385.

851

852 Reich, P. B., Sendall, K. M., Stefanski, A., Rich, R. L., Hobbie, S. E., & Montgomery, R. A.
853 (2018). Effects of climate warming on photosynthesis in boreal tree species depend on soil
854 moisture. *Nature*, 562(7726), 263–267.

855

856 Riihimäki, H., Kemppinen, J., Kopecký, M., & Luoto, M. (2021). Topographic wetness index as
857 a proxy for soil moisture: The importance of flow-routing algorithm and grid resolution. *Water*
858 *Resources Research*, 57(10). <https://doi.org/10.1029/2021wr029871>

859

860 Robinson, D. A., Campbell, C. S., Hopmans, J. W., Hornbuckle, B. K., Jones, S. B., Knight, R.,
861 Ogden, F., Selker, J., & Wendroth, O. (2008). Soil moisture measurement for ecological and

862 hydrological watershed-scale observatories: A review. *Vadose Zone Journal*: VZJ, 7(1), 358–
863 389.

864

865 Romano, N. (2014). Soil moisture at local scale: Measurements and simulations. *Journal of*
866 *Hydrology* , 516, 6–20.

867

868 Rosenbaum, U., Huisman, J. A., Weuthen, A., Vereecken, H., & Bogaen, H. R. (2010). Sensor-
869 to-Sensor Variability of the ECH2O EC-5, TE, and 5TE Sensors in Dielectric Liquids. *Vadose*
870 *Zone Journal*, 9(181-186). <https://doi.org/10.2136/vzj2009.0036>

871

872 Rosenbaum, U., Bogaen, H. R., Herbst, M., Huisman, J. A., Peterson, T. J., Weuthen, A.,
873 Western, A. W., & Vereecken, H. (2012). Seasonal and event dynamics of spatial soil moisture
874 patterns at the small catchment scale. *Water Resources Research*, 48(10).

875

876 le Roux, P. C., Aalto, J., & Luoto, M. (2013). Soil moisture's underestimated role in climate
877 change impact modelling in low-energy systems. *Global Change Biology*, 19(10), 2965–2975.

878

879 Salmivaara, A. 2016. Topographical Wetness Index for Finland, 16m. CSC - IT Center for
880 Science Ltd. <http://urn.fi/urn:nbn:fi:csc-kata20170511114638598124>

881

882 Salmivaara, A. 2020. Cartographic Depth-to-Water (DTW) index map, 2m. CSC - IT Center for
883 Science Ltd. <http://urn.fi/urn:nbn:fi:att:3403a010-b9d0-4948-8f9f-2bc4ca763897>

884

885 Samaniego, L., Thober, S., Kumar, R., Wanders, N., Rakovec, O., Pan, M., Zink, M., Sheffield,
886 J., Wood, E. F., & Marx, A. (2018). Anthropogenic warming exacerbates European soil moisture
887 droughts. *Nature Climate Change*, 8(5), 421–426.

888

889 Seneviratne, S. I., Corti, T., Davin, E. L., Hirschi, M., Jaeger, E. B., Lehner, I., Orlowsky, B., &
890 Teuling, A. J. (2010). Investigating soil moisture–climate interactions in a changing climate: A
891 review. *Earth-Science Reviews*, 99(3-4), 125–161.

892

893 Silvertown, J., Araya, Y. & Gowing, D. (2015), Hydrological niches in terrestrial plant
894 communities: a review. *Journal of Ecology*, 103: 93-108. [https://doi.org/10.1111/1365-](https://doi.org/10.1111/1365-2745.12332)
895 [2745.12332](https://doi.org/10.1111/1365-2745.12332)

896

897 Sorensen, R., and J. Seibert (2007), Effects of DEM resolution on the calculation of
898 topographical indices: TWI and its components, *Journal of Hydrology*, 347(1-2), 79-89.

899

900 Tague, C., Band, L., Kenworthy, S., & Tenebaum, D. (2010). Plot- and watershed-scale soil
901 moisture variability in a humid Piedmont watershed. *Water Resources Research*, 46(12).

902

903 Tarboton, D. G. (1997), A new method for the determination of flow directions and upslope
904 areas in grid digital elevation models, *Water Resources Research*, 33(2), 309– 319,

905 [doi:10.1029/96WR03137](https://doi.org/10.1029/96WR03137)

906

- 907 Teuling, A. J. (2005). Improved understanding of soil moisture variability dynamics.
908 *Geophysical Research Letters*, 32(5). <https://doi.org/10.1029/2004gl021935>
909
- 910 Trimble Inc (2022). <https://geospatial.trimble.com/products-and-solutions/trimble-geo-7x>
911
- 912 Tuttle, S., & Salvucci, G. (2016). Empirical evidence of contrasting soil moisture-precipitation
913 feedbacks across the United States. *Science*, 352(6287), 825–828.
914
- 915 Tyystjärvi, V., Kemppinen, J., Luoto, M., Aalto, T., Markkanen, T., Launiainen, S., Kieloaho,
916 A.-J., & Aalto, J. (2021). Modelling spatio-temporal soil moisture dynamics in mountain tundra.
917 *Hydrological Processes*. <https://doi.org/10.1002/hyp.14450>
918
- 919 Walker, J. P., Willgoose, G. R., & Kalma, J. D. (2004). In situ measurement of soil moisture: a
920 comparison of techniques. *Journal of Hydrology* , 293(1-4), 85–99.
921
- 922 Wang, L., & Liu, H. (2006). An efficient method for identifying and filling surface depressions
923 in digital elevation models for hydrologic analysis and modelling. *International Journal of*
924 *Geographical Information Science*, 20, 193–213. <https://doi.org/10.1080/13658810500433453>
925
- 926 Western, A. W., Grayson, R. B., Blöschl, G., Willgoose, G. R., & McMahon, T. A. (1999).
927 Observed spatial organization of soil moisture and its relation to terrain indices. *Water Resources*
928 *Research*, 35(3), 797–810.
929

930 Western, A. W., Grayson, R. B., & Blöschl, G. (2002). Scaling of Soil Moisture: A Hydrologic
931 Perspective. *Annual Review of Earth and Planetary Sciences*, 30:149–80.

932

933 Wild, J., Kopecký, M., Macek, M., Šanda, M., Jankovec, J., & Haase, T. (2019). Climate at
934 ecologically relevant scales: A new temperature and soil moisture logger for long-term
935 microclimate measurement. *Agricultural and Forest Meteorology*, 268, 40–47.

936

937 Wilson, D. J., Western, A. W., & Grayson, R. B. (2004). Identifying and quantifying sources of
938 variability in temporal and spatial soil moisture observations. *Water Resources Research*, 40(2).
939 <https://doi.org/10.1029/2003wr002306>

940

941

942 Wood, S.N. (2011) Fast stable restricted maximum likelihood and marginal likelihood estimation
943 of semiparametric generalized linear models. *Journal of the Royal Statistical Society (B)* 73(1):3-
944 36

945

946 Yu, L., 1. College of Information and Electrical Engineering, China Agricultural University,
947 Beijing 100083, China, Gao, W., R. Shamsiri, R., Tao, S., Ren, Y., Zhang, Y., Su, G., 2.
948 College of Information Science and Engineering, Shandong Agriculture and Engineering
949 University, Shandong 250100, China, & 3. Leibniz Institute for Agricultural Engineering and
950 Bioeconomy, Potsdam-Bornim 14469, Germany. (2021). Review of research progress on soil
951 moisture sensor technology. *International Journal of Agricultural and Biological Engineering*,
952 14(3), 32–42.

953

954 Zona, D., Lafleur, P. M., Hufkens, K., Gioli, B., Bailey, B., Burba, G., Euskirchen, E. S., Watts,
955 J. D., Arndt, K. A., Farina, M., Kimball, J. S., Heimann, M., Göckede, M., Pallandt, M.,
956 Christensen, T. R., Mastepanov, M., López-Blanco, E., Dolman, A. J., Commane, R. ... Oechel,
957 W. C. (2022). Pan-Arctic soil moisture control on tundra carbon sequestration and plant
958 productivity. *Global Change Biology*, 00, 1– 15. <https://doi.org/10.1111/gcb.16487>

959

960 Ågren, A. M., W. Lidberg, M. Strömgren, J. Ogilvie, and P. A. Arp (2014), Evaluating digital
961 terrain indices for soil wetness mapping - a Swedish case study, *Hydrol Earth Syst Sc*, 18(9),
962 3623-3634.